

# Study of the Reaction of Kidney Collecting Duct Principal Cells to Hypotonic Shock. Experiment and Mathematical Model

A. V. Ilyaskin<sup>a</sup>, G. S. Baturina<sup>a</sup>, D. A. Medvedev<sup>b,c</sup>, A. P. Ershov<sup>b,c</sup>, and E. I. Selenov<sup>a,c</sup>

<sup>a</sup> Institute of Cytology and Genetics, Siberian Branch, Russian Academy of Sciences, Novosibirsk, 630090 Russia

<sup>b</sup> Lavrent'ev Institute of Hydrodynamics, Siberian Branch, Russian Academy of Sciences, Novosibirsk, 630090 Russia

<sup>c</sup> Novosibirsk State University, Novosibirsk, 630090 Russia

E-mail: eugsol@bionet.nsc.ru

Received May 24, 2010; in final form, February 28, 2011

**Abstract**—The reaction of rat kidney collecting duct principal cells to hypotonic shock was studied. The changes in cell relative volume were measured using fluorescent dye calcein, and a mathematical model based on our experimental results was developed. It was shown that regulatory volume decrease is mainly provided by significant release of osmolytes from the cell and decrease of the plasma membrane water permeability. Using our model, we calculated the membrane water permeability and found it to decrease from  $2 \cdot 10^{-1}$  to  $2 \cdot 10^{-2}$  cm/s. We conclude that for effective RVD to occur, a dramatic increase in the membrane permeability to  $K^+$ ,  $Cl^-$  and organic anions is necessary.

**Keywords:** cell volume regulation, mathematical model, kidney

**DOI:** 10.1134/S0006350911030092

## INTRODUCTION

At present, the most promising approach to study the cell properties should combine experiments with mathematical modeling of the process. Existing models of transmembrane osmolyte transport mostly treat the steady states of the cells [1–6]. There is no dynamic model of kidney epithelium cell behavior in hypotonic medium. In this regard, the study of the mechanisms underlying cell volume regulation that are associated with transmembrane water and solute transport is important.

Since the osmotic pressure of tubular fluid around the cells may vary in a broad range, the renal collecting duct principal cells must possess effective mechanism to maintain osmotic homeostasis. A hypotonic medium is most dangerous for cells, because the cell membrane could be disrupted as the consequence of cell swelling.

Water permeability of collecting duct principal cells is provided by the water channels—AQP2 in the apical membrane, and AQP3 and AQP4 in the basolateral membrane [7]. An efficient way of protection from acute swelling in hypotonic conditions could be the decrease of membrane water permeability.

The maintenance of viability and integrity of a cell in hypotonic environment is provided by regulatory cell volume decrease (RVD) mechanisms. According

to many references, RVD includes loss of cell osmolytes such as  $K^+$  and  $Cl^-$  [8–10]. Additionally, there may be efflux of organic substances from cells during RVD [10].

There is no data concerning cells with high water permeability, with characteristic times of swelling and RVD during hypotonic shock of the order of several seconds. For example, Pogorelovs [11] showed that the process of swelling of murine embryo blastomeres lasted for 10 min. The aim of the current study was to create a mathematical model of reaction of renal collecting duct cells to hypotonic challenge on the basis of experimentally measured relative cell volume changes. The analysis of experimental data with the help of the mathematical model allowed us to increase the opportunities of examination of adaptive cellular mechanisms, obtaining quantitative estimates of parameters of the processes for which direct measurement is too complicated.

## EXPERIMENTAL

**Animals.** Wistar rats 60 days old, males and females, were used in experiments. The animals were supplied by Breeding Laboratory of Experimental Animals, Institute of Cytology and Genetics, Novosibirsk, Russia. Rats were kept in individual cages and received standard diet. For standardization of animal state and increasing the osmotic water permeability of the outer medullary collecting duct (OMCD) epithelium prior to beginning of the experiments, rats were subjected to

Translation of the text provided by the authors; some redaction imposed for literacy and comprehensibility.

antidiuresis by water deprivation and providing only dry food for 36 h (hypohydrated animals).

**Collecting duct fragments.** Rats were anesthetized with pentobarbital (50 mg/kg intraperitoneally) and decapitated. Extracted kidneys were placed in ice-cold PBS (pH 7.4), then decapsulated and decorticated. A suspension of collecting duct fragments was prepared in the following way: tissue from the outer medulla zone was squeezed through a needle (0.45 mm i.d.) in ice-cold calcium-free PBS. The resulting suspension was filtered through a nylon mesh, diluted 10 times with Eagle MEM culture medium and centrifuged (100 g, 10 min, 4°C). This suspension was used in experiments as a preparation of OMCD fragments.

**Solutions.** The isotonic solutions used were based on PBS (124 mM NaCl, 4.7 mM Na<sub>2</sub>HPO<sub>4</sub>, 2.7 mM KCl, 1.5 mM KH<sub>2</sub>PO<sub>4</sub>, 0.5 mM MgCl<sub>2</sub>, 1 mM CaCl<sub>2</sub>, 280 mOsmol/L, pH 7.4) containing 1.0 mg/mL glucose. To create osmotic challenges, bath solutions were changed from normal to PBS diluted with distilled water (1 : 1). For medullary substance dispersion, low calcium PBS was used (124 mM NaCl, 4.7 mM Na<sub>2</sub>HPO<sub>4</sub>, 2.7 mM KCl, 1.5 mM KH<sub>2</sub>PO<sub>4</sub>, 0.5 mM MgCl<sub>2</sub>, 0.05 mM CaCl<sub>2</sub>).

**Perfusion chamber and microscopy.** A superfusion chamber was constructed to be mounted on the objective of an upright fluorescent microscope LOMO-R8 (St. Petersburg, Russia). The chamber volume was approximately 50 μL, the flow rate was 25 mL/min, which resulted in complete solution exchange in less than 100 ms, thermal stabilization was at 36.8 ± 0.2°C. The objective (water immersion × 60 magnification, numerical aperture 1.0) was thermally stabilized. Fragments of OMCD in 0.1 mL of MEM were placed on a glass plate and were loaded with Calcein-AM (Invitrogen, CA, USA) (5.0 μM) by incubation for 15 min at 4°C, and then for 25 min at 37°C in 5% CO<sub>2</sub>. The glass plate with fragments of OMCD was positioned on the stage of a microscope. Fluorescence measurements of cell volume were performed by the calcein quenching method as it was previously described [12]. Cell volume changes were expressed as relative values of calcein fluorescence. Calcein fluorescence was measured continuously, through a filter set: 490 nm excitation, 520 nm emission. A photomultiplier detector (PMT-71, Russia) with an adjustable diaphragm was used in order to be able to select the cells of interest in the fragment. Measurements were done with a 14-bit analog-to-digital converter PCL-818HG (Advantech). Data were recorded on PC hard disk.

**Methods of mathematical modeling.** The proposed mathematical model describes transmembrane fluxes of a hypothetical cell which contains Na<sup>+</sup>, K<sup>+</sup>, Cl<sup>-</sup> and organic anion (X) channels, Na<sup>+</sup>/K<sup>+</sup>-pump, K<sup>+</sup>-Cl<sup>-</sup> (KCC) and Na<sup>+</sup>-K<sup>+</sup>-2Cl<sup>-</sup> (NKCC) cotransporters in its membrane. The list of channels and transporters under consideration was chosen according to the

experimental evidence of their expression in membranes of renal collecting duct cells [13–20]. The cell surface area *A* permeable for ions and water was considered to be constant and independent of cell volume changes owing to the low extensibility of lipid bilayer.

The fluxes of osmolytes through ion channels were simulated using the Fick–Planck diffusion equations, with the Goldman–Hodgkin–Katz transformation taken into account [21, 22].

The flux provided by Na<sup>+</sup>/K<sup>+</sup>-pump activity was described by a detailed kinetic scheme utilizing the Hill graphic algorithm [23]. For the reason of the small contribution of this flux to the overall osmolyte loss from the cell during RVD, model parameters of the Na<sup>+</sup>/K<sup>+</sup>-pump were based on the analysis of a stationary state of the enzyme functioning [4, 5].

Transmembrane fluxes through KCC and NKCC cotransporters depended only on transmembrane concentration gradients of ions and were independent of transmembrane potential [24]. These currents were proportional to permeability parameters  $Q_{\text{KCC}}$  and  $Q_{\text{NKCC}}$ .

The calculation of transmembrane potential difference was carried out using the value of membrane capacitance  $C_m$  [6]. In contrast to models that utilize Goldman–Hodgkin–Katz equation and its derivatives [1–5, 25], this approach allows one to avoid the assumed limitation of potential stability ( $dE/dt = 0$ ) while calculating potential difference in the presence of nonzero net transmembrane current [6].

Osmotic water flux was taken into account in the model by the water permeability parameter ( $P_w$ ) and the rate of cell volume change.

In order to estimate the stationary state of the system the values of membrane Na<sup>+</sup>, K<sup>+</sup> and Cl<sup>-</sup> permeability parameters  $P_{\text{Na}}$ ,  $P_{\text{K}}$ ,  $P_{\text{Cl}}$ , cotransporters' permeabilities  $Q_{\text{KCC}}$ ,  $Q_{\text{NKCC}}$  and Na<sup>+</sup>/K<sup>+</sup>-pump density  $N$  were chosen to fit the calculated values of intracellular concentrations [Na<sup>+</sup>]<sub>in</sub>, [K<sup>+</sup>]<sub>in</sub> and [Cl<sup>-</sup>]<sub>in</sub> and resting membrane potential with experimentally measured values for collecting duct cells [26–28]. Parameters were modified in the neighborhood of values taken from [1–6]. Extracellular osmolarity was defined by the sum of Na<sup>+</sup>, K<sup>+</sup> and Cl<sup>-</sup> concentrations according to the experimental protocol, while intracellular osmolarity was determined by the total intracellular Na<sup>+</sup>, K<sup>+</sup>, Cl<sup>-</sup> and organic anion X concentration. The amount of organic anions X was chosen to provide the equality between total intracellular and extracellular osmolyte concentration (280 mM). The mean charge of organic ions  $z$  was fitted to provide approximate electroneutrality of intracellular environment. The main equations, symbols and initial values of variables and parameters of the model are listed in Appendix.

Numerical integration of differential equations used in the model was carried out by Runge–Kutta

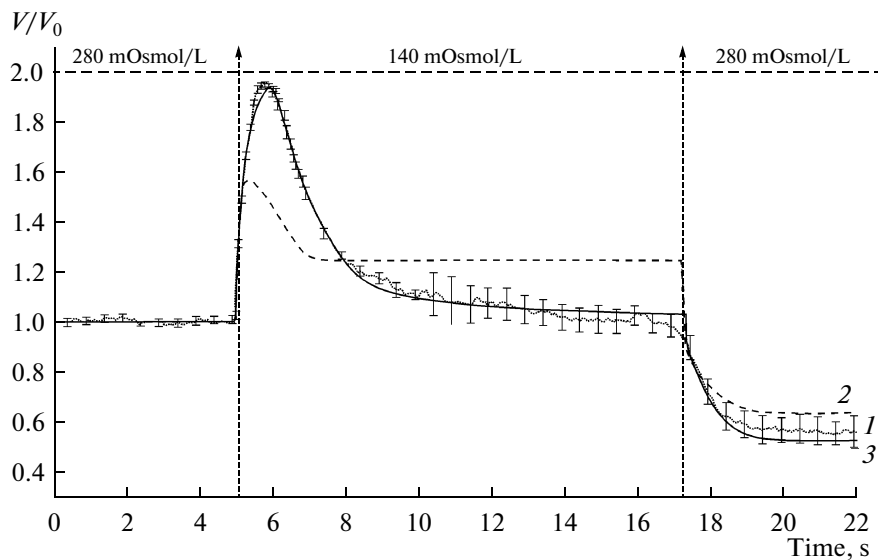


**Fig. 1.** Changes in relative volume  $V/V_0$  of renal principal collecting duct cells during hypotonic challenge in experiment and results of simulations employing approximations of the model with volume dependence. (1) Averaged experimental recordings of calcein fluorescence ( $n = 6$ ) with indication of standard error of mean ( $SE$ ); (2) RVD simulation (zero approximation); (3) RVD simulation (first approximation). The top scale represents the changes of extracellular osmolarity (mOsmol/L).

forth order method. The integration time step  $dt$  was  $10^{-5}$  s in general. This value is much smaller than the characteristic times of the processes modeled. To validate the computations some simulations were performed with tenfold decreased time step ( $10^{-6}$  s), which caused no significant changes. To simulate cell reaction to the hypotonic shock the parameters of water and ion permeability were fitted manually using the fitting criterion between experimental and simulated curves, which was the square root of the sum of the squared relative cell volume differences ( $V/V_0$ ) at each iteration time point:

$$\sqrt{\sum(V_{\text{exp}}/V_{\text{exp}}^0 - V_{\text{mod}}/V_{\text{mod}}^0)^2}. \quad (1)$$

**Statistics.** All values are expressed as mean  $\pm$  standard error ( $M \pm SE$ ). The plotted changes of relative fluorescence were obtained via averaging of the experimental recordings ( $n = 6$ )  $\pm SE$ .

## RESULTS

Figure 1 represents relative cell volume changes during hypotonic shock in experiment. It is evident that hypotonic shock is accompanied by acute increase of cell volume followed by RVD due to the loss of osmotically active substances by the cell. Following the return to the isotonic environment after shock, the steady state volume of cells approximated 60% of the initial volume.

On the basis of experimental data obtained, a mathematical model of OMCD principal cell reaction to the hypotonic challenge was created. Two variants of the model were made with different degree of

approximation (see table). In the simplest variant, the increase of relative cell volume up to 1.3 was set as a trigger of RVD. The simplified mechanism of RVD was accepted, which was simulated by stepwise increase of  $K^+$ ,  $Cl^-$  and organic anion X effluxes. In the model the increase of the plasma membrane permeability was reflected by multiplying the initial values by parameter «gain», the permeability for organic ions was defined as 50% of permeability for potassium ions. The threshold level of 1.3 and gain value were fitted using trial and error method. After the decrease of relative cell volume to 1.3, the initial values of permeability parameters were restored. Such an approach will be referred to as the zero approximation.

One can see that such an approximation simulates the time history of the cell volume rather roughly. Particularly, there are large deviations of the model from experimental cell volume peaks in hypotonic medium (Fig. 1).

Taking into account the presence of ion channels activated by membrane stretch in a cell [30, 31] and the possible influence of mechanical tension of cytoskeleton on the activity of different kinases and G-proteins involved in the cell signaling pathways [32–34], it seems necessary to consider the influence of intracellular signaling systems on the processes of cell volume regulation. To obtain a more appropriate theoretical time course of cell volume, the lag period of osmolyte permeability increase was introduced into the formulae of the model. According to the experimental data, at the beginning of swelling (in 0.9 s) the cell increases its volume like an ideal osmometer, which is consistent with the view that there is no sig-

## Approximation versions of the model

Approximation	Values of permeability parameters		
Zero approximation (threshold parameter – cell volume)	$V/V_0 \leq 1.3$	$V/V_0 > 1.3$	
	$P_K = P_K^0$ $P_{Cl} = P_{Cl}^0$ $P_X = 0$ $Q_{KCC} = Q_{KCC}^0$	$P_K = P_K^0 \times gain^*$ $P_{Cl} = P_{Cl}^0 \times gain$ $P_X = P_K^0 \times gain$ $Q_{KCC} = Q_{KCC}^0 \times gain$	
First approximation (threshold parameter – cell volume, continuous dependence, lag-period 0.9 s)	$V/V_0 \leq 1$	$1 < V/V_0 < 1.3$	$V/V_0 \geq 1.3$
	$P_K = P_K^0$ $P_{Cl} = P_{Cl}^0$ $P_X = 0$ $Q_{KCC} = Q_{KCC}^0$	$P_K = P_K^0 \left( (gain - 1) \left( \frac{(V/V_0 - 1)}{0.3} \right)^2 + 1 \right)$ $P_{Cl} = P_{Cl}^0 \left( (gain - 1) \left( \frac{(V/V_0 - 1)}{0.3} \right)^2 + 1 \right)$ $P_X = P_K^0 \times 0.5 \times gain \left( \frac{(V/V_0 - 1)}{0.3} \right)^2$ $Q_{KCC} = Q_{KCC}^0 \left( (gain - 1) \left( \frac{(V/V_0 - 1)}{0.3} \right)^2 + 1 \right)$	$P_K = P_K^0 \times gain$ $P_{Cl} = P_{Cl}^0 \times gain$ $P_X = P_K^0 \times gain$ $Q_{KCC} = Q_{KCC}^0 \times gain$
Explicit time dependence ( $t = 0$ at the moment of osmolarity change 280 → 140)	$t \leq 0.9$	$0.9 < t < 2.9$ ( $\tau_{high} = 2$ s)	$t \geq 2.9$ ( $\tau_{decay} = 1$ s)
	$P_K = P_K^0$ $P_{Cl} = P_{Cl}^0$ $P_X = 0$ $Q_{KCC} = Q_{KCC}^0$	$P_K = P_K^0 \times gain$ $P_{Cl} = P_{Cl}^0 \times gain$ $P_X = P_K^0 \times gain$ $Q_{KCC} = Q_{KCC}^0 \times gain$	$P_K = P_K^0 (1 + (gain - 1)) e^{[(-t + 2.9)]/\tau_{decay}}$ $P_{Cl} = P_{Cl}^0 (1 + (gain - 1)) e^{[(-t + 2.9)]/\tau_{decay}}$ $P_X = P_K^0 \times gain \times 0.5 e^{[(-t + 2.9)]/\tau_{decay}}$ $Q_{KCC} = Q_{KCC}^0 (1 + (gain - 1)) e^{[(-t + 2.9)]/\tau_{decay}}$

Note:  $gain = 1100$  in all approximation variants.

nificant osmolyte efflux during this period. The next approximation reflects this by the 0.9 s delay of RVD initiation following the change of extracellular osmolarity.

As the stepwise change of permeability is too rough an approximation, a continuous dependence of permeability on cell volume was introduced to overcome the observed discrepancy between calculated and experimental curves. The introduction of a continuous condition allowed us to achieve better agreement of calculated and averaged experimental cell volume time course. The modified model could be called the first approximation model. In this variation of the model, the increase of membrane permeability was described by the implementation of continuous function  $f(V/V_0)$ , which equals unity when  $V/V_0 > 1.3$  and increases from 0 to 1 over the range  $1 < V/V_0 < 1.3$ . Such a dependence represents graduality of the cell reaction to a change of volume, which is natural within the framework of mechanical activation. The function type was chosen from considerations of simplicity and

correspondence with experimental data. Acceptable concordance appeared to be achieved under the parabolic volume dependence over the range  $1 < V/V_0 < 1.3$ . Calculations showed that the first approximation model successfully describes the cell behavior (Fig. 1).

Despite the good agreement with the experiment, the «mechanistic» approach described above is not the only possible one. Moreover, it should be considered as some preliminary oversimplified theory. Mechanical activation does not reflect the whole set of processes taking place in a cell challenged by hypotonic shock. One can speculate that the permeability of cell membrane transporters activated during RVD is guided not by the direct stretching of the membrane but by cell signaling pathways employing a chain of enzymatic reactions that could be considered as a «cell clock». According to such an idea, a new characteristic parameter was introduced in the model, namely the time interval of the high activity of transporters followed by the exponential decrease of permeabilities to the initial level. Permeabilities were expressed as

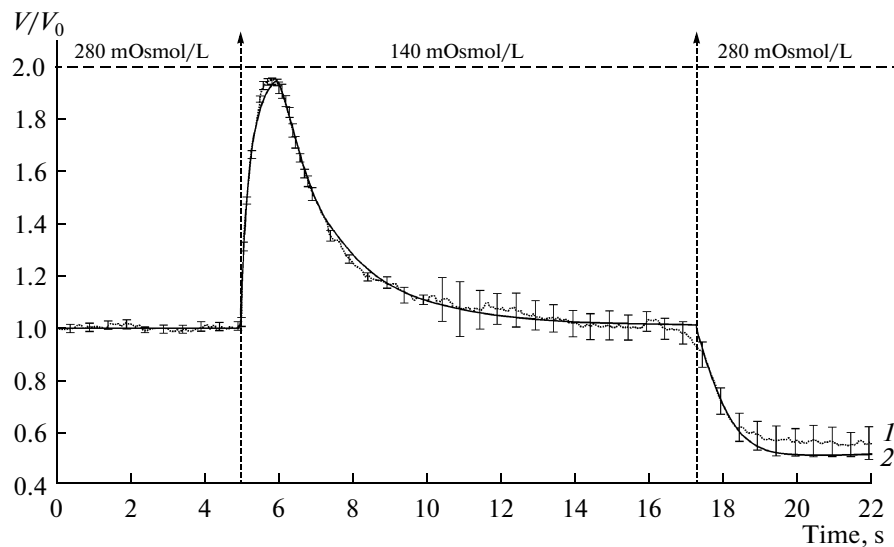


**Fig. 2.** Changes in relative volume  $V/V_0$  of renal principal collecting duct cells during hypotonic challenge in experiment and results of simulations employing the explicit time dependence model. (1) Averaged experimental recordings of calcein fluorescence ( $n = 6$ ) with indication of standard error of mean ( $SE$ ); (2) RVD simulation (explicit time dependence). The top scale represents the changes of extracellular osmolarity (mOsmol/L).

explicit functions of time, formulae used for calculations are given in the table. Besides the amplitude of permeability increase (*gain*), the model contains two variable parameters, which are the duration  $\tau_{\text{high}}$  of the period characterized by elevated permeability of the membrane to osmolytes and the characteristic time of regulatory reaction decay  $\tau_{\text{decay}}$  after the period with high permeability. Modification of the model with explicit time dependence of permeability parameters allowed us to fit the values of parameters for the simulated time course of the relative cell volume to be in the limits of  $SE$  for experimental data (Fig. 2).

Simulation allowed us to estimate the contribution of different ion fluxes to the cell volume decrease. Figure 3 demonstrates that at the beginning of RVD the flux through KCl cotransporter prevails over all other fluxes ( $J_{\text{KCC}}$ ). Also there is a significant contribution of  $\text{K}^+$  and organic anion diffusion fluxes ( $J_{\text{K}}$  and  $J_{\text{X}}$ ). These currents mostly define the equilibrium cell volume in hypotonic environment. It should be noted that the  $\text{Cl}^-$  flux ( $J_{\text{Cl}}$ ) acquires positive meanings (influx) and does not take part in the decrease of intracellular  $\text{Cl}^-$  concentration. Analysis of the results of modeling also allowed us to estimate the changes in the amount of intracellular osmotically active substances caused by the hypotonic shock. It is apparent from the calculation of amounts of intracellular osmolytes that their total content was decreased by 47% in comparison with the initial level ( $2.80 \cdot 10^{-13}$  and  $1.48 \cdot 10^{-13}$  mol/cell before and after the RVD respectively), which is in good agreement with the results of the experiment.

Water permeability changes during the RVD were also estimated with the help of the model. Figure 4 shows the profiles of relative cell volume changes in the explicit time-dependence model and in the experiment. Water permeability parameter was fitted to obtain the minimal value of criterion (1). The following values of water permeability were established:

before the hypotonic shock:  $P_w = 2 \cdot 10^{-1}$  cm/s;

after the hypotonic shock:  $P_w = 2 \cdot 10^{-2}$  cm/s.

The water permeability decrease was assumed to be in the agreement with formula:

$$P_w = P_w^0(0.1 + 0.9 \exp(-t + 0.9)), \quad (2)$$

where  $t = 0$  is a moment when the total concentration of extracellular ions was halved ( $280 \rightarrow 140$  mM). Thus, during the RVD the water permeability coefficient was decreased tenfold. Such a conclusion comes from the analysis of the slope of the part of the cell volume profile where the cell volume decreases following the extracellular osmolarity change from hypotonicity to normotonicity.

## DISCUSSION

The mathematical model describes the ion fluxes across the cell membrane that determine the cell volume changes:  $\text{Na}^+$ ,  $\text{K}^+$ ,  $\text{Cl}^-$ . The organic ions and organic molecules without electric charge are presented as one pool in the model. Good agreement of calculated and experimental data means that it is an acceptable approximation for the present model. The model controlled by the cell volume and that employ-

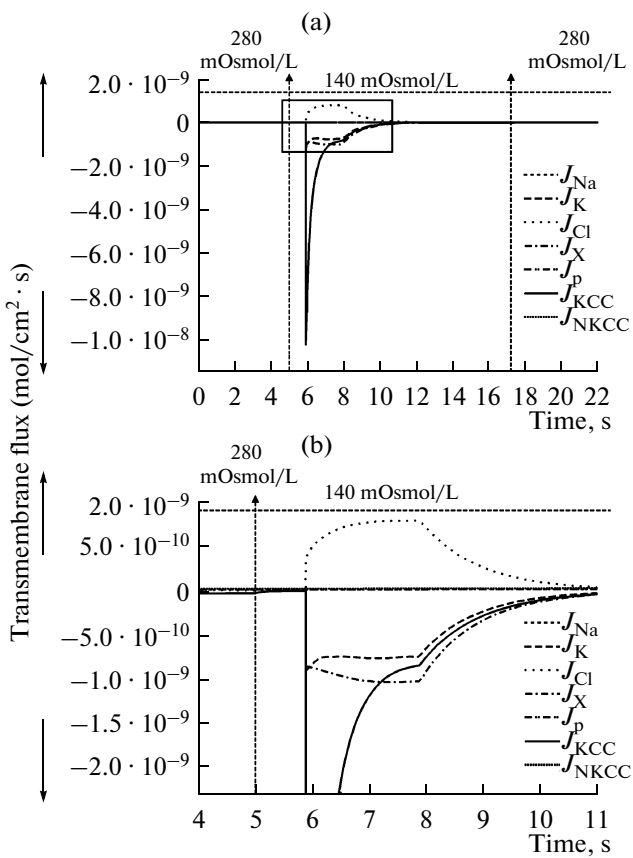


**Fig. 3.** The time dependence of simulated transmembrane ion fluxes ( $\text{mol}/\text{cm}^2 \cdot \text{s}$ ). (a) General ratio of fluxes through different membrane transporters. (b) Scaled-up part of the first graph (marked by rectangular frame) corresponding to the RVD reaction. The top scale represents the changes of extracellular osmolarity (mOsmol/L). Arrows along the ordinate axis represent the direction of fluxes: in the cell – upward arrow; out of the cell – downward arrow.

ing the activity time gave similar results. Nevertheless, the model in which the cell volume is a control parameter looks too mechanistic. Obviously, mechanistic activation does not reflect the whole complex of processes in the cells which undergo osmotic shock. At least the biochemical reactions triggered by changing concentration of signal molecules or/and plasma membrane electric potential are important too [8, 10]. The model in which the activity time is a control parameter may be regarded as a preliminary material for a more thorough future theory. In that version of model, the important parameters are the characteristic times of hypothetical regulatory processes that control the activity of plasma membrane transporters of the cell.

One can suppose that the permeability of the transporters that participate in the RVD reaction is controlled through a complicated enzymatic reaction chain. This pathway may be regarded as a “cell clock”. Then the permeabilities were expressed as explicit

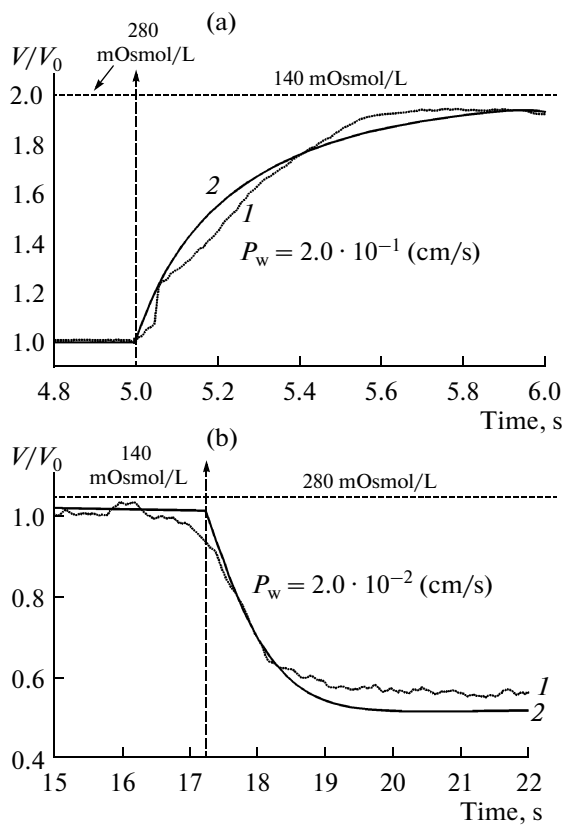


**Fig. 4.** The time dependence of the relative cell volume in experiment and model (line 2 – model, line 1 – experiment) in the following cases: (a) cell swelling in hypotonic conditions ( $280 \rightarrow 140$ ); (b) cell shrinkage in normotonic conditions ( $140 \rightarrow 280$ ). The top scale represents the changes of extracellular osmolarity (mOsmol/L).

functions of time. This approach gives some useful information. With accuracy limited by the error of experimental measurements, the duration of the high-activity period of transporters and the lifetime accounting for the subsequent exponential decrease of high permeability to the initial level were introduced as parameters of the model. In all the variants of our model it was necessary to increase the permeability parameters by three orders of magnitude to get a good agreement with experimental data.

The mathematical modeling evaluates the ion fluxes across cell membrane that determine the cell volume decrease. It can be seen in Fig. 3 that the flux through the KCl cotransporter ( $J_{\text{KCC}}$ ) prevails at the beginning of the RVD. The contribution of fluxes of  $\text{K}^+$  and of organic anions X ( $J_{\text{K}}$  and  $J_{\text{X}}$ ) in maintenance of cell volume in hypotonic medium is also considerable. It should be noted the flux of chloride ions ( $J_{\text{Cl}}$ ) is directed inside the cell. Nevertheless, the total intracellular  $\text{Cl}^-$  content decreases, because the exit through the KCl cotransporter surpasses this influx. Analysis of the time course of cell volume and the ion

**Table 1.** Symbols of parameters and variables used in the model

Parameter	Symbol
Cell volume	$V$
Cell surface area	$A$
Integration step	$dt$
Membrane $\text{Na}^+$ permeability	$P_{\text{Na}}$
Membrane $\text{K}^+$ permeability	$P_{\text{K}}$
Membrane $\text{Cl}^-$ permeability	$P_{\text{Cl}}$
Membrane X permeability	$P_X$
Membrane osmotic water permeability	$P_w$
Permeability parameter of KCC cotransporter	$Q_{\text{KCC}}$
Permeability parameter of NKCC cotransporter	$Q_{\text{NKCC}}$
Intracellular concentration and amount of $\text{Na}^+$ , respectively	$[\text{Na}^+]_{\text{in}}, n_{\text{Na}}$
Intracellular concentration and amount of $\text{K}^+$	$[\text{K}^+]_{\text{in}}, n_{\text{K}}$
Intracellular concentration and amount of $\text{Cl}^-$	$[\text{Cl}^-]_{\text{in}}, n_{\text{Cl}}$
Intracellular concentration and amount of organic anions X	$n_X$
Transmembrane potential difference	$E_m$
Total Na/K-pump membrane density	$N$
Extracellular $\text{Na}^+$ concentration	$[\text{Na}^+]_{\text{out}}$
Extracellular $\text{K}^+$ concentration	$[\text{K}^+]_{\text{out}}$
Extracellular $\text{Cl}^-$ concentration	$[\text{Cl}^-]_{\text{out}}$
Total extracellular concentration of osmolytes	$\Pi_e$
Membrane capacitance	$C_m$
Mean organic osmolyte valency	$z$
Partial molar volume of water	$V_w$
Faraday's constant	$F$
Absolute temperature	$T$
Gas constant	$R$

currents indicates that the model gives quite an adequate description of the temporal order of events that constitute RVD. The mathematical modeling allowed us to estimate the changes of intracellular amounts of selected ions. The calculation of the osmolyte intracellular contents in our model confirms the opinion that the RVD is mainly performed by significant release of  $\text{K}^+$  and  $\text{Cl}^-$  from the cell.

Conclusions made on the basis of mathematical modeling of the cell response to hypotonic shock require experimental verification. The advantage of our current approach is the possibility of experimental revision of the parameters of the mathematical model. If further investigations show that the model gives

results consistent with the experiment, our approach may be employed in order to determine the functions of membrane transporters and the temporal RVD processes under hypotonic conditions of various cell types.

## APPENDIX

The mathematical model describes the time course of cell volume  $V$ , amounts of osmolytes  $\text{Na}^+$ ,  $\text{K}^+$ ,  $\text{Cl}^-$  and of organic anions X (in mole) in the cell, and the time dependence of electric transmembrane potential difference ( $E_m$ ):

$$\frac{dV}{dt} = (AV_w P_w) \left[ \frac{n_{\text{Na}} + n_{\text{K}} + n_{\text{Cl}} + n_X}{V} - \Pi_e \right], \quad (3)$$

$$E_m(t) = F(n_{\text{Na}} + n_{\text{K}} + n_{\text{Cl}} + z n_X)/C_m/A, \quad (4)$$

$$\frac{dn_{\text{Na}}}{dt} = A[-3J_p + J_{\text{Na}} + J_{\text{NKCC}}], \quad (5)$$

$$\frac{dn_{\text{Na}}}{dt} = A[2J_p + J_{\text{K}} + J_{\text{KCC}} + J_{\text{NKCC}}], \quad (6)$$

$$\frac{dn_{\text{Cl}}}{dt} = A[J_{\text{Cl}} + 2J_{\text{NKCC}} + J_{\text{KCC}}], \quad (7)$$

$$\frac{dn_X}{dt} = AJ_X. \quad (8)$$

Passive ion fluxes were modeled as follows [21, 22]:

$$J_{\text{Na}} = P_{\text{Na}} \varepsilon(u) \left[ [\text{Na}^+]_{\text{out}} \exp\left(-\frac{u}{2}\right) - \left(\frac{n_{\text{Na}}}{V}\right) \exp\left(\frac{u}{2}\right) \right], \quad (9)$$

$$J_{\text{K}} = P_{\text{K}} \varepsilon(u) \left[ [\text{K}^+]_{\text{out}} \exp\left(-\frac{u}{2}\right) - \left(\frac{n_{\text{K}}}{V}\right) \exp\left(\frac{u}{2}\right) \right], \quad (10)$$

$$J_{\text{Cl}} = P_{\text{Cl}} \varepsilon(u) \left[ [\text{Cl}^-]_{\text{out}} \exp\left(\frac{u}{2}\right) - \left(\frac{n_{\text{Cl}}}{V}\right) \exp\left(-\frac{u}{2}\right) \right], \quad (11)$$

where  $u = FE_m/RT$  and  $\varepsilon(u) = u/[\exp(u/2) - \exp(-u/2)]$ .

The outward flux of organic anions is defined similarly taking into account their extracellular concentration,  $X=0$ :

$$J_X = -P_X \varepsilon(u) \left[ \left(\frac{n_X}{V}\right) \exp\left(\frac{uz}{2}\right) \right]. \quad (12)$$

The  $\text{Na}^+/\text{K}^+$ -pump activity was described by the detailed kinetic scheme that is reported in [4, 5, 29] and calculates the pump flux  $J_p$  as:

$$J_p = \left(\frac{1}{\Sigma}\right)(\alpha - \beta), \quad (13)$$

where  $\alpha$  is the function of forward rate constants,  $\beta$  is the function of backward rate constants and  $\Sigma$  is the function of all rate constants and the ligand concentrations implemented in the kinetic scheme.

**Table 2.** Initial values of parameters and variables used in the model of collecting duct principal cell

Parameter	Symbol	Value
Cell volume	$V_0$	$1 \cdot 10^{-9} \text{ cm}^3$
Cell surface area	$A$	$1 \cdot 10^{-5} \text{ cm}^2$
Membrane $\text{Na}^+$ permeability	$P_{\text{Na}}$	$3 \cdot 10^{-8} \text{ cm/s}$
Membrane $\text{K}^+$ permeability	$P_{\text{K}}^0$	$2 \cdot 10^{-8} \text{ cm/s}$
Membrane $\text{Cl}^-$ permeability	$P_{\text{Cl}}^0$	$2 \cdot 10^{-8} \text{ cm/s}$
Membrane osmotic water permeability	$P_w^0$	$2 \cdot 10^{-1} \text{ cm/s}$
Permeability parameter of KCC cotransporter	$Q_{\text{KCC}}^0$	$8 \cdot 10^{-8} \text{ cm}^4 \text{ mol}^{-1} \text{ s}^{-1}$
Permeability parameter NKCC cotransporter	$Q_{\text{NKCC}}$	$1.9 \cdot 10^6 \text{ cm}^{10} \text{ mol}^{-3} \text{ s}^{-1}$
Intracellular $\text{Na}^+$ concentration	$[\text{Na}^+]_{\text{in}}$	$2.05 \cdot 10^{-5} \text{ mol/cm}^3$
Intracellular $\text{K}^+$ concentration	$[\text{K}^+]_{\text{in}}$	$1.40 \cdot 10^{-4} \text{ mol/cm}^3$
Intracellular $\text{Cl}^-$ concentration	$[\text{Cl}^-]_{\text{in}}$	$3.63 \cdot 10^{-5} \text{ mol/cm}^3$
Intracellular amount of organic anions	$n_X$	$8.3 \cdot 10^{-14} \text{ mol}$
Transmembrane potential difference	$E_m$	$-0.051 \text{ V}$
Total $\text{Na}^+/\text{K}^+$ -pump membrane density	$N$	$3 \cdot 10^{-13} \text{ mol/cm}^2$
Extracellular $\text{Na}^+$ concentration	$[\text{Na}^+]_{\text{out}}$	$1.35 \cdot 10^{-4} \text{ mol/cm}^3$
Extracellular $\text{K}^+$ concentration	$[\text{K}^+]_{\text{out}}$	$5 \cdot 10^{-6} \text{ mol/cm}^3$
Extracellular $\text{Cl}^-$ concentration	$[\text{Cl}^-]_{\text{out}}$	$1.4 \cdot 10^{-4} \text{ mol/cm}^3$
Total extracellular concentration of osmolytes	$\Pi_e$	$2.8 \cdot 10^{-4} \text{ mol/cm}^3$
Membrane capacitance	$C_m$	$7 \cdot 10^{-7} \text{ F/cm}^2$
Mean organic osmolyte valency	$Z$	$-1.5$

Since one working cycle of  $\text{Na}^+/\text{K}^+$ -pump includes the transfer of three  $\text{Na}^+$  out and two  $\text{K}^+$  in a cell, the fluxes of  $\text{Na}^+$  and  $\text{K}^+$  provided by ATPase activity equal  $-3J_p$  and  $2J_p$ , respectively.

Fluxes through the co-transporters (NKCC and KCC) are modeled using the following equations:

$$J_{\text{NKCC}} = Q_{\text{NKCC}}([\text{Na}^+]_{\text{out}}[\text{K}^+]_{\text{out}}[\text{Cl}^-]_{\text{out}}^2 - [\text{Na}^+]_{\text{in}}[\text{K}^+]_{\text{in}}[\text{Cl}^-]_{\text{in}}^2), \quad (14)$$

$$J_{\text{KCC}} = Q_{\text{KCC}}([\text{K}^+]_{\text{out}}[\text{Cl}^-]_{\text{out}} - [\text{K}^+]_{\text{in}}[\text{Cl}^-]_{\text{in}}). \quad (15)$$

These fluxes utilize the permeability parameters  $Q_{\text{NKCC}}$  and  $Q_{\text{KCC}}$  [5, 6]. They are independent of  $E_m$  in agreement with experimental evidence [24] and depend only on the transmembrane ion concentration gradients. The initial values of the model parameters are listed in Table A2.

According to the experimental conditions, the hypotonic shock was modeled by decreasing twofold the values of intracellular concentrations, i.e.

$[\text{Na}^+]_{\text{out}}/2$ ,  $[\text{K}^+]_{\text{out}}/2$ ,  $[\text{Cl}^-]_{\text{out}}/2$ . The fitting of the values of model parameters was performed in a way that would maximize the correspondence between averaged experimental and simulated data points of the relative cell volume time course using criterion (1).

The reaction of RVD was modeled by triggering the complex of regulatory events that included: rapid increase of membrane permeability to  $\text{K}^+$  and  $\text{Cl}^-$  ions; outward flux of organic anions X.

## ACKNOWLEDGMENTS

This work was supported by RFBR (08-04-00541, 09-04-00197) and grant #58 of SB RAS.

## REFERENCES

1. C. Armstrong, PNAS **100**, 6257 (2003).
2. R. Jacob, D. Piwnica-Worms, R. Horres, M. Lieberman, J. Gen. Physiol. **83**, 47 (1984).
3. R. Moreton, J. Exp. Biol. **51**, 181 (1969).

4. J. Hernandez, J. Fischbarg, L. S. Liebovitch, *J. Theor. Biol.* **137**, 113 (1989).
5. J. Hernandez, S. Chifflet, *J. Membr. Biol.* **176**, 41 (2000).
6. J. Fraser, *J. Physiol.* **559** (2), 459 (2004).
7. S. Nielsen et al., *Physiol. Rev.* **82**, 205 (2002).
8. F. Lang et al., *Physiol. Rev.* **78**, 247 (1998).
9. K. Strange, *Advan. Physiol. Edu.* **28**, 155 (2004).
10. E. Hoffmann, I. Lambert, S. Pedersen, *Physiol. Rev.* **89**, 193 (2009).
11. A.G. Pogorelov, V.N. Pogorelova, *Biophysics*, **54** (3), 336 (2009).
12. E. I. Solenov, H. Watanabe, G. T. Manley, A. S. Verkman, *Am. J. Physiol. Cell. Physiol.* **286**, C426 (2004).
13. J. Legato, M. A. Knepper, *Physiol. Genomics* **13**, 179 (2003).
14. M. Reif, S. Troutman, J. Schafer, *J. Clin. Invest.* **77**, 1291 (1986).
15. G. Frindt, L. Palmer, *Am. J. Physiol. Renal. Fluid. Electrolyte. Physiol.* **252**, F458 (1987).
16. G. Frindt, L. Palmer, *Am. J. Physiol. Renal. Fluid. Electrolyte. Physiol.* **256**, F143 (1989).
17. W. Wang, S. Hebert, G. Giebisch, *Annu. Rev. Physiol.* **59**, 413 (1997).
18. S. Muto, *Physiol. Rev.* **81** (1), 85 (2001).
19. M. Haas, B. Forbush, *Annu. Rev. Physiol.* **62**, 515 (2000).
20. S. Wall, M. Fischer, P. Mehta, K. Hassell, S. Park, *Am. J. Physiol. Renal. Physiol.* **280**, 913 (2001).
21. D. E. Goldman, *J. Gen. Physiol.* **27**, 37 (1943).
22. A. Hodgkin, B. Katz, *J. Physiol.* **108**, 37 (1949).
23. T. Hill, New York: Academic Press, pp. 1–32 (1977).
24. P. Lauf, N. Adragna, *Cell. Physiol. Biochem.* **10**, 341 (2000).
25. L. Mullins, K. Noda, *J. Gen. Physiol.* **47**, 117 (1963).
26. J. Gifford, J. Galla, R. Luke, R. Rick, *Am. J. Physiol.* **259**, F778 (1990).
27. C. Pappas, B. Koeppen, *Am. J. Physiol.* **263**, F1004 (1992).
28. B. Stanton, *Am. J. Physiol.* **256**, F862 (1989).
29. I. Chapman, E. Johnson, J. Kootsey, *J. Membrane. Biol.* **74**, 139 (1983).
30. L. Wang, G. Ding, Q. Gu, W. Schwarz, *Eur. Biophys. J.* **39** (5), 757 (2010).
31. A. Dyrda et al., *PLoS ONE* **5** (2), 9447 (2010).
32. S. Lee, Z. Shen, D. Robinson, S. Briggs, R. Firtel, *Mol. Biol. Cell. Epub ahead of print* (2010).
33. R. Kaunas, P. Nguyen, P. Usami, S. Chien, *PNAS* **102** (44), 15895 (2005).
34. H. Multhaupt, A. Yoneda, J. Whiteford, et al., *J. Physiol. Pharm.* **60**, 31 (2009).